Chapter 12

Cell Interaction Analysis by Imaging Flow Cytometry

Cristian Payés, José A. Rodríguez, Sherree Friend and Gustavo Helguera

Additional information is available at the end of the chapter

http://dx.doi.org/10.5772/51147

1. Introduction

Many processes such as cell adhesion, tissue development, cellular communication, inflammation, tumor metastasis, and microbial infection require direct interactions between cells. Some cell-cell interactions are transient, as is the case of the contacts between cells of the immune system, the interactions of white blood cells to malignant cells or to sites of tissue inflammation. These events often entail structural alterations in the point of contact of the cells involved, and may involve the fusion, transfer or exchange of material between the cells; which occur in a scale that is suited for optical microscopy analysis. However, due to its low throughput nature, microscopy often suffers from acquisition bias and limited statistical power. Moreover, because the data is typically analyzed in a qualitative manner, it is difficult to obtain standardized results. Strong scientific conclusions demand objective collection of large amounts of relevant information that can be analyzed in a quantitative, standardized, and statistically robust manner. Flow cytometry overcomes these problems but reduces the rich information available via optical microscopy to a set of intensity measurements. By combining high speed automated image acquisition with quantitative image analysis, Multispectral Imaging Flow Cytometry (MIFC) provides all the elements required for discriminating cells based on intensity and appearance in a standardized and statistical manner. In recent years, the application of this technology for the analysis of cell-cell interaction has multiplied, in particular in the field of immunology, allowing the observation and quantification of events in a way that could not be achieved before. Although studies investigating the interaction of pathogens with host cells have been conducted using MIFC in combination with confocal fluorescence microscopy and immuno cytochemistry microscopy [1], here we will only address the interaction of cells belonging to the same species, therefore host-pathogen cell-cell interactions are beyond the scope of the current manuscript.

2. Combining microscopic imaging and flow cytometry to characterize cell-cell interactions

The characterization of cells and subcellular components using methods that detect fluorescent labels is invaluable to biology. The expansion and adoption of fluorescence microscopy techniques in biology has made routine the detailed characterization of fluorescently labeled structures in single cells. As the modern standard of fluorescence-based microscopic imaging, confocal microscopy is capable of rendering the diffraction-limited three-dimensional representation of a single fluorescently labeled cell; taking up to several minutes to do so. By generating high-resolution images of one or a few cells a minute, fluorescence microscopy is limited in its throughput. In contrast, flow cytometry has revolutionized the identification and measurement of fluorescently labeled cells and subcellular elements via the rapid quantification of bulk fluorescent signal from single cells on a population-wide scale. In fact, modern flow cytometers can routinely measure hundreds of thousands of cells per second [2].

Both fluorescence microscopes and flow cytometers are capable of obtaining multi-spectral measurements of cells. This ability to simultaneously identify multiple fluorescent labels within a sample has facilitated the characterization of many cellular components in multiple cell populations in a single sample [2]. However, biologists have traditionally been forced to chose between the detection of fluorescence signals in cells at high resolution but with low throughput via microscopic imaging, and the rapid quantification of bulk fluorescent signal in a heterogeneous population of cells by flow cytometry [3]. These technologies have thus become largely complementary to each other, supplying information from both ends of the resolution-throughput spectrum.

Given the individual benefits of microscopic imaging and flow cytometry, the ideal measurement should leverage and combine the unique abilities of both technologies. The statistical power of flow cytometry would then be infused with detailed cellular imagery, with each individual point in a dataset representing the detailed image of a single fluorescently labeled cell or group of cells. Until recently, several technical challenges have limited the existence of a robust imaging flow cytometer capable of producing the high resolution fluorescent images expected from a microscope as well as the high throughput measurement associated with flow cytometry. MIFC instruments are now commercially available (see www.amnis.com). [4].

2.1. Elements of multispectral imaging flow cytometry (MIFC)

This chapter describes their use for the characterization of cell-cell interactions: Section 2.1 provides a technical overview of MIFC instruments, section 2.2 provides an overview of the methodology used to characterize cell-cell interactions using MIFC, section 3 describes a specific example of use of MIFC to measure and characterize cell-cell interactions, namely antibody-dependent cell-mediated cytotoxicity, while section 4 covers a broad range of examples in which MIFC has assisted in the characterization of a variety of cell-cell interactions.

2.1.1. Brief history of MIFC

Shortly after the development of flow cytometry, attempts at infusing the technology with microscopic imaging began [3]. The first attempts intended to add morphological information to fluorescence intensity measurements for each object encountered. To do this, slit cyto-fluorometers simultaneously recorded low-resolution measurements of object shapes and bulk fluorescence [5]. Alternatively optical impedance measurements and side-scatter were combined with bulk fluorescence signal to give a rough estimate of particle size and granularity, rapidly and reliably. Strobe lighting combined with fast CCD cameras have allowed for true microscopic imaging of cells in flow [5]. However, these approaches, including scanning, tracking, and strobe illumination techniques, have been limited in their ability to reliably generate high-resolution images of all cells in a flow stream with sufficient fluorescence sensitivity [3]. Recently an imaging system that overcomes most of these barriers has become commercially available and has demonstrated the ability to provide high spatial resolution images, high fluorescence sensitivity, reliable high-throughput acquisition, and the simultaneous analysis of fluorescence signals at various wavelengths [4]. With this system, a new dimension has been effectively added to conventional microscopic analysis, allowing for the execution of previously intractable experiments and the development of completely new forms of analysis.

2.1.2. The MIFC instrument

Multispectral Imaging Flow Cytometry combines the high throughput capability of the flow cytometer with the imaging capability of the microscope. Hydrodyanamically focused cells are trans-illuminated by a brightfield light source and orthogonally by laser light. [4]. Fluorescence emissions, scattered, and transmitted light from the cells are collected using a high numerical aperture objective. The collected light is directed through a spectral decomposition element which places light of different spectral bands into separate positions (channels) on the CCD camera in spatial alignment to each other. [6]. The camera records these images and stores them for subsequent analysis. These systems are capable of measuring over 1000 individual events every second, translating to hundreds of thousands of cells in just a few minutes [4]. Moreover, each cell is comprised of up to 12 images (one for each imaging channel); well over a million images in a five-minute time span [4].

2.1.3. High resolution images in MIFC

When imaging cells moving rapidly within a flow channel, the relative motion of the cells with respect to the detector must be accounted for. A method termed time-delay integration [4] detects the velocity of cells with respect to the detector (a CCD camera) and synchronizes the integration of signal intensity on a per pixel basis with the cell velocity over the length of the camera. This is equivalent to panning the detector alongside passerby cells with a matching speed, in effect neutralizing the relative motion of the cells, which prevents streaking and increases the sensitivity and resolution of the detector [4].

2.1.4. Extended depth of field using MIFC

As with most microscopic imaging systems, proper focus is essential for obtaining high-quality images. This is especially true for cells traveling along a flow channel whose size allows for movement of cells in the direction perpendicular to the flow path, or for cells significantly larger than the depth of focus of the optics used [6]. In such cases, signal from parts of cells that lie outside the focal volume can be blurred or altogether lost. To counteract this effect during standard microscopic analysis of cells, several focal volumes can be collected and assembled or added to generate an effective focal volume that encompasses the entire cell. The imaging flow cytometer employs autofocusing and extended depth of field methods to recover what would normally be out of focus signal, effectively extending the range of a single focal volume from four micrometers to sixteen micrometers at 40X magnification [6].

2.1.5. Multi-parameter image processing using MIFC

While microscopic analysis offers a rich array of parameters that can be interpreted from a single cell, the sampling of enough cells to find statistical significance in these observations may not be tractable. Flow cytometers overcome this statistical limitation by collecting large sample sizes. By quickly sampling thousands of cells within minutes or seconds, MIFC generates a wealth of information in two spatial dimensions for each of its independent imaging channels [4]. The spatial resolution of the images is used to compute hundreds of photometric and morphometric features for every cell. [7]. Thus, MIFC instantly increases the amount of information available for each cell over 1000-fold [3, 4]. In traditional flow cytometry experiments, this information is collapsed to a single point on a scatterplot for each cell detected.

The photometric and morphometric parameters are calculated post acquisition of the images using algorithms that take into account location and intensity of the fluorescence, darkfield and brightfield images. Cell populations can be categorized using multiple parameters. Parameters are available that measure size, shape, texture, signal strength and location. Masks are available that focus the calculations to specific regions of the cells. This means cell morphology can be quantified, allowing cell populations to be categorized using their true structure rather than simple size and granularity measurements typical of flow cytometry analyses. Determinations that are performed by standard flow cytometry such as measurement of intracellular cell calcium or evaluation of tight junctions between cells could also be resolved and analyzed with this technology. Additionally, localization and co-localization of signals from multiple labels can be associated to subcellular compartments such as the nucleus, cell surface, or visible organelles. To identify truly spatially co-existent signals within a subcellular compartment, cells can be measured with or without the use of extended depth of focus technology [6].

2.2. Cell-cell interactions characterized using MIFC

2.2.1. Measuring rare events using MIFC

Many phenomena in biology, including cell-cell interactions, occur as fleeting events or in very low frequencies. The difficulty in characterizing these events is typically overcome

by sampling a large number of cells using a high-throughput approach such as flow cytometry. In such a case, the key is to sample as many cells as possible so that the number of rare events observed allows for meaningful information to be extracted from them. A conventional microscope would not serve this purpose well, as it would take an intractable amount of time to find a large enough number of events to make valuable conclusions. However, since MIFC can measure hundreds of thousands of cells from a single population within minutes, even events that only occur at a rate lower than one percent can be investigated [3]. In such a case, when only one out of every one thousand cells forms a cell-cell complex, up to five hundred complexes could be measured within a matter of minutes.

2.2.2. Detecting a multi-cell complex using MIFC

The application of extended depth of field to MIFC is particularly important for the accurate detection of cell-cell interactions. The size of most cells lies outside the range of the standard focal volume [6]. Detecting cell-cell interactions when limited by a narrow focal volume would prove to be a debilitating challenge. A cube, whose sides are each 20-30 micrometers in length, depending on the cell type, can represent two or more interconnected cells (Figure 1). In this case, a four micrometer focal volume could likely miss one of the cells altogether and would rarely intercept the cell-cell complex at an appropriate focal plane to resolve the junction between the cells [6]. In contrast, the sixteen-micrometer focal volume offered by the use of the extended depth of field element covers largely the entire volume and should easily resolve the cell-cell junction (Figure 1).

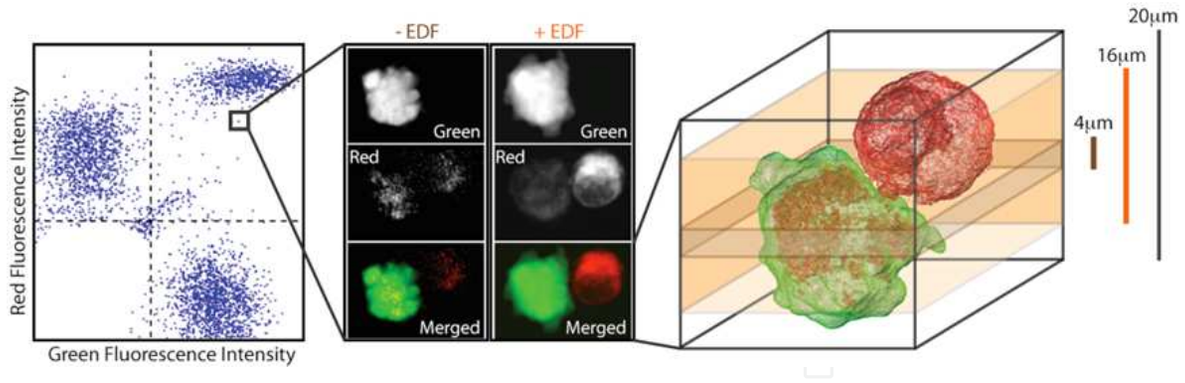

Figure 1. Identification of rare cell-cell interactions using multi-spectral imaging flow cytometry. From two cell populations labelled independently with green and red fluorescent dyes, a scatterplot is shown (left) in which single or dual labelled specimens can be identified. From a single event in the scatterplot, images can be recalled, having been obtained simultaneously for each of the fluorescent channels. Using the extended depth of field technology, the entire complex of one green and one red labelled cell can be imaged as shown in the montage (middle). Without the EDF technology a limited depth of field might not identify the cell-cell interaction or might do so only partially. The range of the interaction volume captured with the aid of the EDF technology is illustrated in the three dimensional cell-cell interaction volume rendered (right).

2.2.3. Multi-color analysis of cell-cell interactions using MIFC

The multi-spectral measurement of bulk cell fluorescence has revolutionized flow cytometry. Populations of cells can be identified as being labeled by unique combinations of fluorescent dyes, implying powerful relationships between the molecules being labeled in single cell populations and the relative quantities in which they are present in these cells [2]. Likewise, MIFC can simultaneously acquire up to twelve independent imaging channels at a time, allowing for a variety of molecular associations to be probed within a single cell population [4]. However, instead of just measuring bulk fluorescence intensity, spatial correlations can be quantitatively determined for each of the fluorescent labels measured (Figure 1). The spatial distribution and co-segregation of each of these independently measured labels can be used to quantitatively paint a true multi-spectral image of a cell population [4]. To achieve quantitative results with single pixel accuracy, corrections are applied to the pixel data for subpixel spatial registration and spectral overlap of the fluorochromes used. Correction values are obtained through routine instrument calibration and the collection of single color compensation controls [4].

The nature of cell-cell interactions necessitates the disambiguation of components from two physically linked cells. Until recently, the true characterization of these interactions required high-resolution fluorescence microscopy or electron micrograph analysis. The challenge lies in spatially separating the signal obtained from each interacting partner. Using spectrally distinct fluorescent labels satisfies this requirement, since emitted signals can be identified from independent cell populations, which when detected in coexistence indicates a physical interaction between the two cell types. Using MIFC, cell-cell interactions can be corroborated by morphometric analysis of the distribution of fluorescence signal and visual analysis of brightfield images [3]. More importantly, both the interaction region and the crossing of signal between interacting cells can also be identified using MIFC by tracking the spatial distribution of fluorophores unique to each interacting partner. Direct interactions can be quantified either as a result of spatial co-segregation of signal or direct signal overlap, and are limited only by the spatial resolution of the optical configuration used (Figure 1).

3. MIFC to study cell interaction in antibody dependent cell-mediated cytotoxicity

The use of MIFC based methodologies for the characterization of cell-cell interactions is enjoying rapid growth. This is true in part because, as described in section 2 of this chapter, MIFC instruments have the unique ability to characterize transient or rare cell-cell interactions in mixed cell populations. In this section we discuss the use of MIFC to quantitatively characterize a particular type of cell-mediated cytotoxicity, termed antibody-dependent cell-mediated cytotoxicity (ADCC), in which immune system cells and their targets on the move exhibit short-lived physical interactions that result in the large-scale loss of target cells.

ADCC is an immune defense mechanism mediated by cells in which effectors cells of the immune system expressing Fc gamma receptors interact with the Fc domain of antibodies

bound to antigens present on the surface of the target cell and actively induce their cytotoxicity. This process requires the formation of a direct connection between both cells, also referred as a cytotoxic synapse, in which there is a transient cytoplasmic contact and mutual exchange of membrane lipids between the effector and target cell [8]. The clinical success of many recombinant antibodies used in the therapy of cancer such as the chimeric anti-CD20 IgG1 rituximab and the humanized anti-HER2 IgG1 trastuzumab has been associated in great extent to the mechanism of ADCC [9, 10]. The determination of ADCC is usually performed using methods that quantify the release of a traceable compound from target cells upon their death, or methods that detect the coexistence of different traceable compounds normally found in only effector or target cell populations. Traditionally radiodosimetry, colorimetry, spectrometry, or flow cytometry have been used to measure these events. However, MIFC has also been used to quantitatively characterize individual ADCC events in mixed populations of immune effector cells and cancer cells, in the presence of a clinically relevant therapeutic antibody [11]. The human monocyte cell line U-937 was used as an effector cell population, and fluorescently labeled with CMTPX red dye, while the human Burkitt's B-cell non-Hodgkin's lymphoma (NHL) cell line Ramos were fluorescently labeled with CFSE green dye. The nuclei of these cells were also fluorescently labeled with the DRAQ5 dye. The two populations of labeled cells were mixed in the presence or the absence of rituximab, to characterize transient effector-target cell interaction events using the ImageStream (multispectral imaging flow cytometer) (Figure 2). MIFC data were processed using the IDEAS software package (Amnis, Seattle WA), which identified individual effector and target cells as well as effector-target cell complexes. The apoptotic index of each cell was also determined through the quantitation of nuclear morphometric parameters (based on the two dimensional distribution of DRAQ5 label within the cell nuclei), including nuclear texture, condensation, and fragmentation (Figure 3). MIFC facilitated the simultaneous analysis of large image datasets representing thousands of events within a measured population. For this analysis a nuclear mask was generated, containing pixels with intensity values in the upper 40% of the intensity range of the DRAQ5 image for $CFSE^+$ (target) or $CMTPX^+$ (effector) cells. Based on this strategy the percentage of apoptotic target cells was determined. These were the apoptotic $CFSE^+$ cells as a fraction of the total number of $CFSE^+$ cells. Since this metric could also be applied to effector cells, the apoptotic status of effector cells within a mixed population could also be quantified. This methodology offers a more complete perspective of cell death within mixed populations, particularly given that current methods ignore the status of the effector cells in the ADCC activity and may overlook some potential toxicity triggered on effector cells. Based on the results presented, MIFC appeared to improve the accuracy with which the biological activity of therapeutic antibody candidates can be evaluated, indicating that the use of traditional methods may provide misleading estimates of the therapeutic benefit of these antibodies.

In addition to providing a quantitative assessment of cell death for each cell in a population, the transfer of cytoplasmic material from effector to target cells was also quantified from images of double-positive ($CMTPX^+$,$CFSE^+$) events. These were identified in multispectral images as the presence of CMTPX dye from the effector cells within the area marked by

CFSE labeled target cells. In the presence of rituximab, a significant increase in the proportion of target cells containing CMTPX signal covering 25-50% of the target cells was detected (Figure 4). In contrast, no cases of signal transfer into effector cells was observed, suggesting that the transfer of cell contents in effector-target pairs is unidirectional, from effector to target cells, as would be expected in cases of ADCC activity.

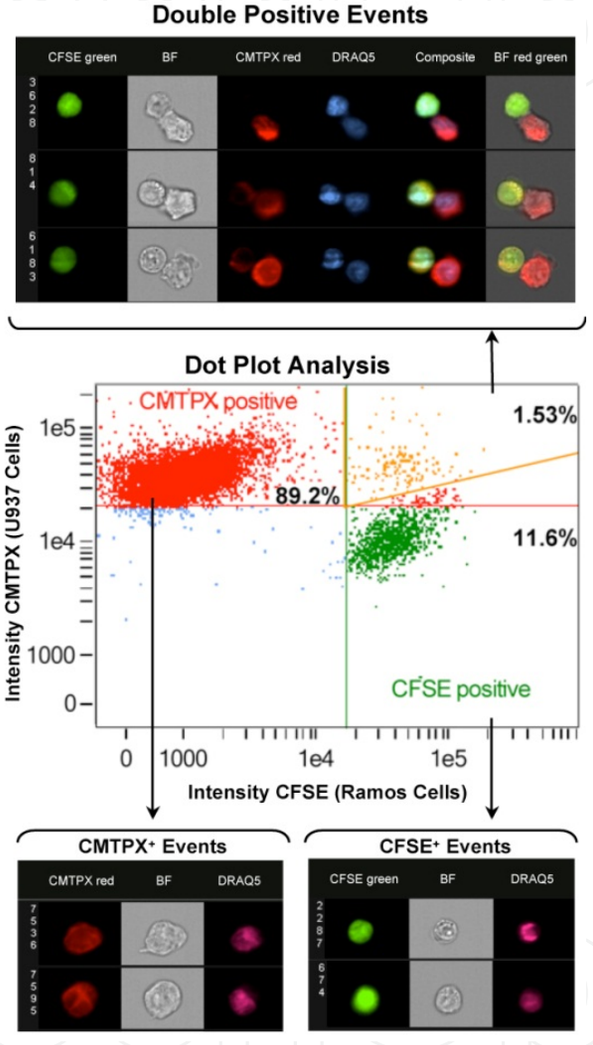

Figure 2. Identification of effector and target cells by imaging flow cytometry. Standard dot plot analysis was used to determine red and green fluorescence intensity in U-937 human monocyte effector cells labeled red with the CMTPX fluorochrome co-incubated for 2 h with Ramos human Burkitt's B-cell NHL target cells labeled green with the CFSE fluorochrome (5:1—E:T ratio) in the presence of 5 μg/ml rituximab. After incubation, cells were fixed and nuclei stained with the DRAQ5 dye. Samples were run in the ImageStream and imagery acquired for 10,000 events. In the middle of the figure we show the dot plot of the treatment with the percentage of events $CMTPX^+$ in the upper left quadrant, $CFSE^+$ in the bottom right quadrant, and $CMTPX^+/CFSE^+$ in the top right quadrant. Above the dot plot we show representative imagery of double positive events from the upper right quadrant of the dot plot with CFSE fluorescence (CFSE green), brightfield (BF), CMTPX fluorescence (CMTPX red), DRAQ5 fluorescence (DRAQ5), CFSE, CMTPX, and DRAQ5 fluorescence (composite), and brightfield, CFSE and

CMTPX fluorescence (BF red green). Below left we show representative imagery of single U-937 cells CMTPX positive from the upper left quadrant of the dot plot with CMTPX red, BF, and DRAQ5 pictures. And finally, below right we show representative imagery of single Ramos cells CFSE positive from the bottom right quadrant of the dot plot with CFSE green, BF, and DRAQ5 pictures. Figure is reprinted from Helguera et al. 2011, with permission from Elsevier.

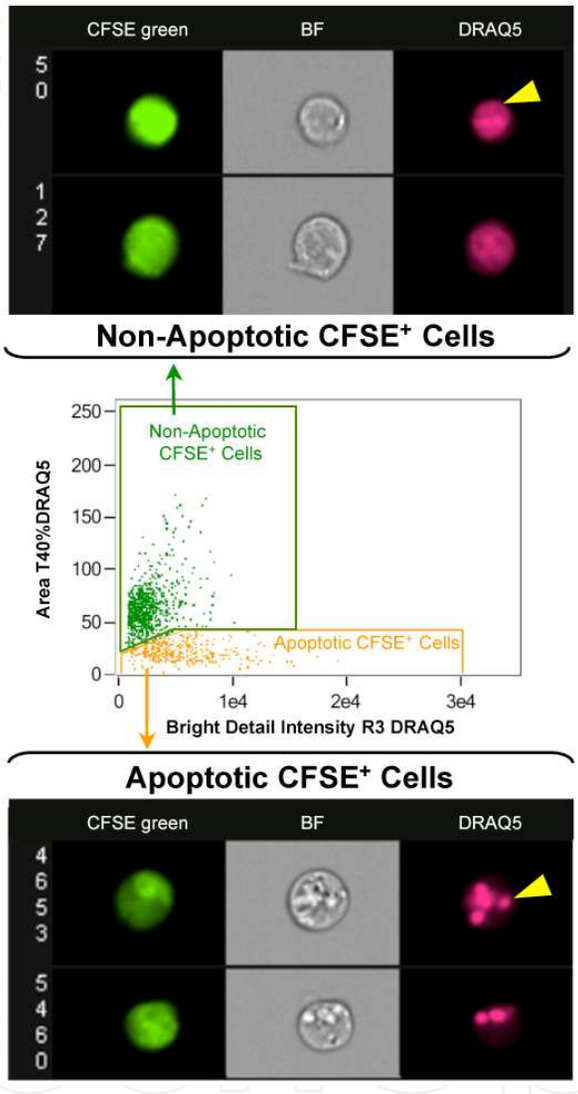

Figure 3. Determination of apoptotic index by nuclear morphology. At the center is a bivariate plot analysis using the IDEAS® software showing Area threshold 40% DRAQ5 intensity versus bright detail intensity R3 DRAQ5 parameters of Ramos cells labeled with CFSE co-incubated for 2 h with U-937 effector cells in the presence of 5 μg/ml rituximab. The non-apoptotic Ramos CFSE+ cells are gated in green. Sample CFSE, brightfield and DRAQ5 imagery are shown on top, with the yellow triangle pointing to the homogeneous nucleus stained with DRAQ5 typical of non-apoptotic cells. Apoptotic CFSE+ cells are shown in orange, and representative CFSE, brightfield and DRAQ5 images are shown on the bottom, with the yellow triangle pointing to the nucleus fragmented and intensely stained with DRAQ5, typical of apoptotic cells. Note also in BF images the change in morphology, with intense granularity of the cytoplasm. Figure is reprinted from Helguera et al. 2011, with permission from Elsevier.

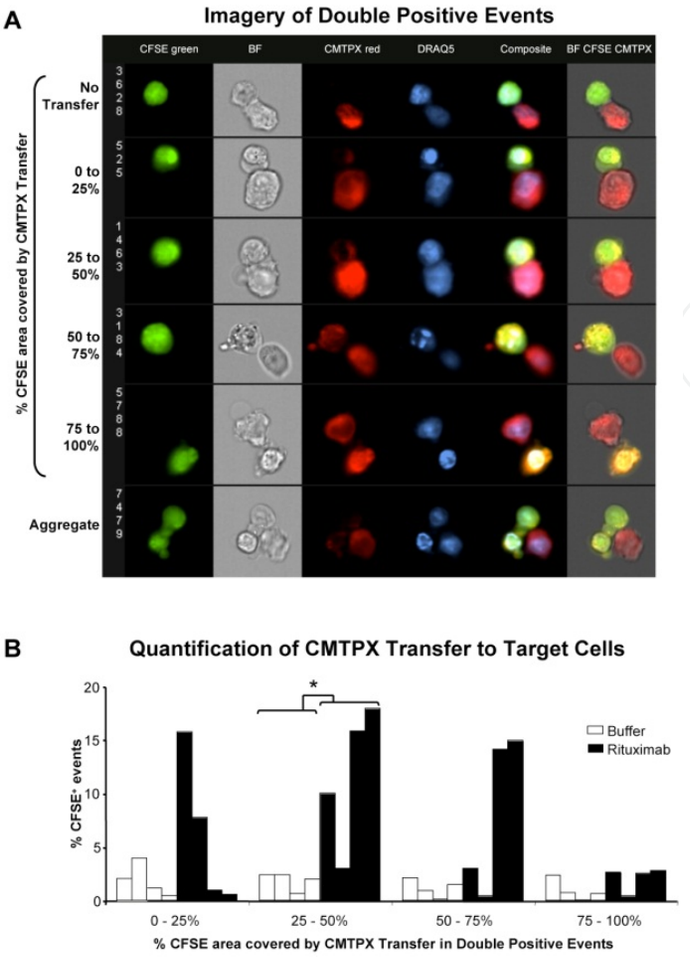

Figure 4. Analysis of cytoplasmic transfer from effector cells to target cells in double positive events. We used an ImageStream multispectral system and acquired a total of 10,000 events to study the double positive events containing Ramos cells stained with CFSE and U-937 cells stained with CMTPX after incubation for 1 h in the absence and presence of rituximab. Panel A shows imagery of double positive events including CFSE fluorescence, brightfield, CMTPX fluorescence, DRAQ5 fluorescence, a composite image of fluorescent stain, and an overlay of brightfield, red and green fluorescence. In the descending rows we show representative imagery of double positive events with increasing percentage of green ($CFSE^+$) masked region covered by red ($CMTPX^+$) mask, evidence of cytoplasmic transfer from effector to target cells. At the bottom we show representative imagery of an aggregate of multiple target cells and an effector cell. Panel B shows the percentage of $CFSE^+$ events with different percentages of CFSE area covered by CMTPX fluorescence comparing buffer treatment (open bars) and rituximab (black bars). Each bar corresponds to different experiments and (*) t-test $p \leq 0.05$. Figure is reprinted from Helguera et al. 2011, with permission from Elsevier.

Similarly, images of double positive events could be analyzed to quantify the contact area between effector and target cells in the context of phagocytic events or antibody-dependent cell mediated phagocytosis (ADCP). The determination of phagocytosis of target cells by effector cells was obtained by measuring the absolute distance between the center of the CMTPX and CFSE signals of cell complexes, which was calculated using the Delta Centroid XY (DC) feature of the IDEAS package. Phagocytic events, in which effector cells surround or engulf target cells, exhibit significantly lower DC values compared to conjugation events.

In events where the DC measurement approaches a 3 μm threshold (smaller than the radius of CMTPX and CFSE images) cell complexes were considered to be in the phagocytosis/internalization range. This was performed for all complexes observed in a mixed population, providing quantitative histogram plots for condition comparisons (Figure 5). In summary, MIFC can be used to simultaneously quantify and visualize the apoptotic index of effector and target cells, together with the transfer of labeled cytoplasmic contents from effector to target cells and the qualitative and quantitative analysis of phagocytic events favored by antibodies, providing a more comprehensive analysis of ADCC activity compared to standard techniques. A related phenomenon observed in the context of cell-cell interaction mediated by antibodies, is the transfer of membrane fragments from a target cell to an acceptor cell, in a process called trogocytosis or "cell nibbling". In this process, the effector cell internalizes the antibody, the captured receptor and membrane fragments from the target cell. This activity was studied for three therapeutic antibodies, the anti-CD20 rituximab, anti-EGFR cetuximab and anti-HER2 trastuzumab using MIFC [12]. MIFC was used to visualize the transfer of portions of the outer membrane of the human B-cell line Raji and its associated protein CD20, into the effector cell line THP-1, in the presence of rituximab. In this case, the membranes of Raji cells were labeled with the PKH26 dye, preincubated in the presence of Alexa 488 labeled rituximab and incubated with monocytic THP-1 cells that were labeled with anti-CD11b and anti-CD14 antibodies coupled to PE-Cy5. Under these conditions, MIFC was performed to visualize and quantify the presence of both PHK26 signal and Alexa 488 labeled rituximab in THP-1 cells alone or complexed with Raji cells, as evidence of receptor and lipid transfer from the target to the effector cell in the process of trogocytosis [12].

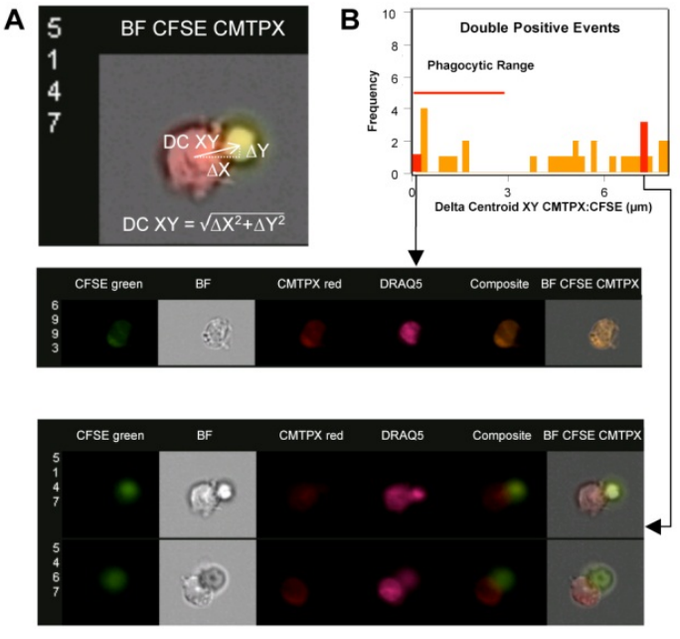

Figure 5. Delta centroid image analysis to identify phagocytosis in double positive events. Panel A shows a composite image of brightfield, CFSE, and CMTPX fluorescence in a double positive event of U-937 effector cells and Ramos target cells incubated for 2 h in the presence of 5 μg/ml rituximab. Superimposed is the vector used to calculate the distance between the centers of the masks of the

effector and the target cell. At the bottom of the image is the equation to calculate the delta centroid XY. Panel B shows a frequency histogram of the delta centroid XY distances of the double positive events. We set a threshold of 3 μm for the delta centroid XY as the phagocytic range, to identify phagocytic events. Below we show imagery of an event inside the phagocytic range in which there is overlapping of green and red signal. At the bottom we show imagery of events in which there is just contact of effector and target cells, resulting in the delta centroid distance equaling the sum of the radii of the green and red fluorescent events (values well beyond the phagocytic range). Figure is reprinted from Helguera et al. 2011, with permission from Elsevier.

4. Other applications of MIFC for the determination of cell-cell interaction

As described in section 3, MIFC offers an in-depth quantitation of previously overlooked aspects of cell-cell interactions that occur as part of ADCC. Likewise, the use of MIFC for the quantification and characterization of cell-cell interactions occurring as a result of a broad range of biological phenomena is expanding our understanding of these events in new and therapeutically meaningful ways. These include cell death arbitrated by other cells, the formation of cell complexes to propagate signals or activate cell populations via the presentation or detection of molecules on cells, the uptake or transfer of cellular materials, the formation of the immunological synapse, and the aggregation of cells to form clusters, plaques, or functional complexes. Cases in which the use of MIFC has led to significant insight into the molecular mechanisms of these phenomena are discussed in this section (Table 1).

Event visualized	Cell types (species)	Identified Marker	Fluorophores (wave length)	Reference
Transfer of Cellular Components	Plasmacytoid dendritic cells (pDC) (human) Monocyte derived dendritic cells (MDDC) (human)	Cell membrane Cytoplasm BDCA-2 CD-123	CFSE (Ex./Em. 492/517nm) PKH67 (Ex./Em. 490/502 nm) PE (Ex./Em. 496/578 nm)	[20]
Transfer of Cellular Components	Raji cells line (from B cells) (human) THP-1 monocytes cells (human)	Cell membrane CD20	PKH26 (Ex./Em. 490/502 nm) Alexa Fluor 488 (Ex./Em. 495/519nm) PE-Cy5 (Ex./Em. 496/785 nm)	[11]
Immunological Synapse	3B11 T hybridoma (mouse) LK35.2 B cells line (mouse)	CD3 LFA-1 F-actin DNA	TexasRed (Ex./Em. 589/615 nm) FITC (Ex./Em. 496/519 nm) Alexa Fluor 568 (Ex./Em. 578/603 nm) Hoechst 33342 (Ex./Em. 350/461 nm)	[15]
Immunological Synapse	T cells (human) Macrophage (human)	Lck CD3 DNA	Alexa Fluor 546 (Ex./Em. 554/570 nm) PE-Alexa Fluor 610 (Ex./Em. 488/628 nm) DRAQ5 (Ex./Em. 631/660 nm)	[14]

Event visualized	Cell types (species)	Identified Marker	Fluorophores (wave length)	Reference
Cell-cell interaction	Mast cells (MCs) (human) Eosinophils (Eos) (human)	Cytoplasm	CFSE (Ex./Em. 492/517nm)	[13]
Cell Aggregate Formation	Regulatory T cells (Tregs) (human) Bone marrow-derived Dendritic cells (BMDCs) (human) Conventional T cells (Tcon) (human)	Cell membrane Cytoplasm CD4 CD11c CD25 IL-2	Alexa Fluor 488 (Ex./Em. 495/519nm) Alexa Fluor 405 (Ex./Em. 401/425nm) Alexa Fluor 633 (Ex./Em. 632/647 nm) Alexa Fluor 647 (Ex./Em. 650/668 nm)	[21]
Cell Aggregate Formation	Leukocytes (human) PBMC (human) of patients with sickle cell disease and healthy individuals	CD45 Glycophorin A (GPA)	FITC (Ex./Em. 496/519 nm) PE (Ex./Em. 496/578 nm)	[23]
Immunological Synapse	$CD4^+$ T cells (mouse) B cells loaded with an antigenic peptide (mouse)	TCRβ LFA-1 DNA	Alexa Fluor 488 (Ex./Em. 495/519nm) PE (Ex./Em. 565/578 nm) 7-AAD (Ex./Em. 546/647 nm)	[16]
ADCC, Apoptosis, Phagocytosis, Transfer of Cellular Components	Ramos cell line, Burkitt's B-cell lymphoma (human) U-937 cell line monocyte (human)	Cytoplasm DNA	CFSE (Ex./Em. 492/517nm) CMTPX (Ex./Em. 577/602nm) DRAQ5 (Ex./Em. 631/660 nm)	[10]
Cell aggregates	Leukocytes (human) with/without CD62 or CD162	CD14 CD36 CD45 DNA	FITC (Ex./Em. 496/519 nm) ECD (Ex./Em. 595/660 nm) PE (Ex./Em. 496/578 nm) DRAQ5 (Ex./Em. 631/660 nm)	[22]
Transfer of Cellular Components	Activated $CD4^+$T cells (human) NK cells (human)	CD3 CD4 CD56 Granzyme K Perforin	Not reported	[10]
Immunological Synapse	1934.4 T cells Antigen presenting cells (APCs) (human)	LFA-1 TCRβ DNA	FITC (Ex./Em. 496/519 nm) PE-TexasRed (Ex./Em. 488⁄615nm) Hoechst 33342 (Ex./Em. 350/461 nm)	[17]

Table 1. Applications of MIFC in cell-cell interaction

4.1. Analysis of the immunological synapse and antigen presentation

The modulation of cells associated with an immune response often requires a direct cell-cell interaction, in some cases via the formation of an immune synapse. In such cases, MIFC has facilitated the quantification of cross talk between different populations of immune cells [13]. In particular, MIFC has been used to evaluate the interaction between Mast cells (MCs) and eosinophils (Eos), key effector cells of an allergic reaction. MIFC was used to identify direct intercellular MC–Eos communication during an allergic response and whether this interaction exerts functional bidirectional changes on the cells. The evaluation of intercellular MC-Eos conjugation was performed by MIFC using a protocol designed to estimate immunological synapse formation. Human cord blood CB (cord blood) -derived MCs were pre-labeled with CFSE (carboxyfluorescein diacetate succinimidyl ester), and mixed with peripheral blood Eos (PB–Eos). Control MC or Eos monocultures were held under similar conditions. To distinguish homotypic from heterotypic couples, CFSE-intensity was used as the parameter: CFSE-high conjugates were MC-MC pairs, CFSE-low events were interacting MC-Eos, and CFSE-negative couples were Eos-Eos pairs. Each population was individually observed for side-scatter and bright-field parameters, so as to eliminate cell debris and irrelevant events. The study demonstrated that MIFC could identify homotypic MC–MC or Eos–Eos pairs in monocultures, as well as the preferential formation of heterotypic MC–Eos couples in co-cultures. These could be directly visualized in Multispectral images, in which overlapping bright field and CFSE label could be quantified, showing the percentage of conjugation between the cells with bar graph. The authors concluded that the high MC–Eos binding rates detected in vitro suggested that this cell–cell contact may be influential during chronic states [13].

Antigen-presenting cells (APC) activate T lymphocytes via the formation of an immunological synapse. In the process of adaptive immune response, APCs present antigenic peptides via MHC molecules to T lymphocytes. This is required to activate the T-cells. The physical contact between these cells results in the polarization of adhesion and cell signaling molecules to the interface between them. MIFC can visualize and quantify the recruitment of CD3 and Lck signaling molecules during the evolution of an immune synapse [14]. Activated primary human T cells mixed with anti-CD3- coated macrophage targets and labeled with both a nuclear dye (DRAQ5) and T cell specific markers, identifying Lck (Alexa 546) and CD3 (PE Alexa 610). Multispectral images from labeled events were analyzed using two independent algorithmic functions to identify the area of the immunological synapse in T cell/APC conjugates: The Valley function, which identifies the dimmest area between two nuclei, and the Interface function, that identifies the site of contact between two cells and selects only the T cell $CD3^+$ area of the T cell/APC synapse. The Valley function can measure the translocation of proteins derived from both the effector and target cell to the immunological synapse, while the Interface function can selectively locate proteins derived from any of the immune cells. Both analytical approaches were used in combination to detect a time dependent increase in the formation of cell conjugates with mature synapses, revealing that the efficiency of conjugate formation and Lck trafficking to the immunological synapse are calcium dependent. At early times and before adding

calcium, fewer than 10% of the conjugates showed both CD3 and Lck concentrated at the immunological synapse. Minutes after calcium was added, approximately 50% of the immunological synapses had matured with both Lck and CD3 accumulating at the interface, although each with its own dynamics [14]. At the T cell/APC interface, the formation of a mature immune synapse involves the accumulation of surface receptors, as well as intracellular signaling and scaffolding molecules defined by clustering of the TCR/CD3 complex at the center of the contact zone (central supramolecular activation cluster, cSMAC), surrounded by a second cluster containing LFA-1 (peripheral SMAC, pSMAC). MIFC implemented through the ImageStream system has been used to study the kinetics of receptor accumulation and immune synapse maturation at the contact zone of 3B11 T cells and LK35.2 B cell couples [15]. In these studies, the interaction between 3B11 T cells and peptide-loaded LK35.2 cells was evaluated. The cell populations were mixed to allow for conjugate formation labeled with molecules detecting CD3 or LFA-1, anti-CD3-biotin plus streptavidin Texas Red and anti-CD18-FITC respectively, F-actin with Phalloidin (Tetramethylrhodamine B isothiocyanate) and Hoechst- 33342 using a nuclear dye. Clustering of CD3 (cSMAC), LFA-1 (pSMAC), and F-actin (pSMAC) were then analyzed using MIFC. The contact zone between 3B11 T and LK35.2 cells was defined as the events with T-cell/B-cell pairs and a Hoechst dye dependent valley mask between the cell pairs. The immune synapse mask was the result of the combination of the valley mask with a T-cell mask that was based on the distribution of CD3 signal. In the absence of presented peptides, most T cells displayed a rather homogeneous surface distribution of CD3 and LFA-1 molecules on their surface as observed by multispectral images of individual events. In contrast, the presence of peptides resulted in the recruitment of both CD3 and LFA-1 signal to the contact zone. A time course study showed that the enrichment of both CD3 and LFA-1 in the contact zone forming the mature synapse, peaked after 30 min of incubation in the presence of the antigenic peptide, decreasing thereafter, but stayed significantly above the level obtained without antigenic peptide. Interestingly, the amount of F-actin in the contact zone, which is crucial for the avidity regulation of integrins, increased over time. The ion chelator EDTA, an inhibitor of both integrin function and TCR/CD3-dependent calcium influx, abolished formation of a mature immune synapse. While the LFA-1 inhibitor, BIRT377 interfered with the accumulation of both LFA-1 and CD3 at the T-cell/B-cell interface and, concomitantly, disturbed mature immune synapse formation [15].

The process of antigen presentation in the context of APC/T cell pairs is compounded by the dual nature of this interaction. T cells are also required to continuously scan DCs presenting a variety of peptides and only be activated in the presence of foreign antigens. To better understand this complex process, MIFC has been used to directly quantify the potency of the immune synapse between T cells and APCs [16]. Recruitment of molecular markers to the intercellular contact zone of APC/T cell pairs was analyzed using MIFC. Because T cell receptor β (TCRβ) and lymphocyte function antigen-1 (LFA-1) are potent activators of immune synapse formation, the authors labeled TCRβ and LFA-1 and measured the enrichment of both markers in the cell-cell interacting domain. The authors isolated CD4 T cells from mice and mixed them with B cells loaded with an antigenic peptide as APCs. The

formation of T–B cell conjugates was detected using MIFC, based on the labeling of independent cell populations with anti-TCRβ Alexa Fluor 488, or phycoerythrin-labeled anti– LFA-1 antibody (2D7), and the DNA marker 7-AAD. Complex formation was identified as the co-existence of TCRβ and LFA-1 signals within a multispectral image. No enrichment of TCR and LFA-1 in the intercellular contact zone was observed in the absence of antigenic peptides. While in the presence of peptide, T cells from mice containing normal numbers of cDCs specifically rearranged TCR and LFA-1, resulting in immune synapse generation. TCR and LFA-1 recruitment peaked at 20–30 min after initiation of T cell– APC contact; however, T cells from DC-depleted mice failed to reorganize TCR and LFA-1, resulting in lack of immune synapse maturation even in the presence of peptide [16].

Similarly, in order to study the correlation of the development of binding forces between T-cells and APCs with the maturation of immune synapse, the kinetics of immune synapse formation was studied using MIFC [17]. As a measure of immune synapse formation, the kinetics of accumulation of T-cell receptor (TCR) and LFA-1 at the interphase of conjugates between murine 1934.4 T cells and APCs were determined by MIFC. APCs (L.Au and L.Au.ICAM-1) cells were loaded with MBP-peptide, and mixed with 1934.4 T cells to allow for immune synapse formation. Cells were labeled with CD18-FITC specific for LFA-1, or TCRβ-biotin plus Streptavidin-PE-TXred specific for the TCR, and their nuclei labeled with the Hoechst dye 33342. An extensive redistribution of LFA-1 and TCR on L.Au.ICAM-1/1934.4 conjugates were observed using MIFC in the presence of antigenic peptide. However, in the absence of peptide, LFA-1 and TCR remained evenly distributed over the T cell surface. Likewise, in complexes of peptide-pulsed L.Au cells and 1934.4 T cells, no redistribution of LFA-1 and TCR molecules to the contact zone was observed. Kinetic studies revealed an increase of mature immune synapse at 15 min post conjugate formation, where mature immune synapse formation could be inhibited with anti-LFA-1 antibody, which correlated with the binding forces measured using cell force microscopy by the authors [17]. These studies are a clear demonstration of the combined advantage of using MIFC over standard flow cytometry or fluorescence microscopy, since MIFC is uniquely capable of objectively and rapidly quantifying the complex distribution of molecules in the contact zone between T cells and APCs for T-cell/APC pairs within a mixed population.

4.2. Phagocytosis of cells and cellular fragments

Some types of dendritic cells possess the ability to take up cellular components from other cells, phagocytose apoptotic bodies or entire cells, and to sample surface components of neighboring live cells via scavenger receptors in a mechanism known as cell nibbling or trogocytosis [18, 19], while other DCs are also known for their ability to generate and release exosomes to mediate cellular interactions. MIFC has been used to investigate the internalization of cellular components between interacting plasmacytoid dendritic cells (pDC) derived from blood, with HSV-infected and uninfected monocyte derived dendritic cells (MDDC) [20]. For these studies, BDCA-2-PE labeled pDC prepared from human PBMC were co-cultured with uninfected or HSV-infected MDDC labeled with CFSE (5,6-carboxyfluorescein diacetate succinimidyl ester), a cytoplasmic marker, or with PKH67, a

green fluorescent lipophilic dye that labels cell membranes. From multispectral images obtained using MIFC, morphometric and photometric parameters for each cell were determined. From these parameters, pDC were quantitatively shown to preferentially associate with and take up membrane from HSV-infected MDDC cells labeled with PKH67. Moreover, the uptake of cytoplasmic components was directly observed and quantified, showing that pDC preferentially take up cellular material from HSV-infected MDDC cells labeled with CFSE. These studies suggest that both PKH67 and CFSE labeling are suitable for analysis of cellular uptake to evaluate cell-cell interactions using MIFC [20].

4.3. Multi-cell clustering and aggregates

While MIFC technology offers a number of advantages over standard detection method for quantifying the behavior of cell pairs, its ability is not limited to two or a few cells. Regulatory T cells (Tregs) are important effectors of immune tolerance; however the signaling molecules influencing their suppressive activity have yet to be fully characterized. MIFC is being used as an important tool to elucidate Treg activity via the quantification and visualization of cell-cell interactions between Tregs and a cytoplasmic factor involved in T cell activation [21]. In these studies, $CD4^{+}CD25^{+}$Tregs from mice were labeled with anti-CD4 Alexa 488, while bone marrow-derived dendritic cells (BMDCs) were labeled with anti-CD11c Alexa 405. Using this labeling scheme, the formation of BMDC-Tregs conjugates was quantified, the complexes scored according to the number of Tregs (1, 2 or 3) attached to the BMDCs. Analysis of multispectral images showed that the presence of antigenic peptides favored the formation of cell complexes, as did the absence of the cytoplasmic tyrosine phosphatase Src homology region 2 domain-containing phosphatase 1 (SHP-1). The presence of cell complexes with a third cell population of conventional T cells (Tcons) labeled with Alexa 647, and of the cells expressing the cytokine IL-2 was also identified [21].

MIFC technology has also been used to study the cellular composition of cell aggregates, as is the case during the formation of rosettes by the adhesion of platelets and leukocytes [22]. CD36 is frequently used as a marker of monocytes, erythrocytes, or platelets in clinical cytometry, while antibodies binding to CD36 may induce platelet activation and formation of platelet's rosettes on leukocytes. This frequently results in the false identification of expression of platelet markers on white blood cells. MIFC analysis has been used to visualize, quantify, and further confirm platelet rosetting on leukocytes after CD36 activation, and the application of anti-CD162 and anti-CD62 antibodies to prevent the formation of these complexes [22]. Using the ''Spot Count'' function of the IDEAS software applied to multispectral images acquired using MIFC, a direct relation between the number of adherent platelets and CD36-FITC intensity for neutrophils, monocytes and lymphocytes was discovered. The number of particles on the surface of neutrophils could be directly counted by analyzing morphological features of detected cells. Among the neutrophils, 64% exhibited at least one particle on their surface, ranging from 1 to 12 particles for FITC fluorescent cells in presence of CD36 mAbs. Using the same morphological analysis, inhibition of platelet adhesion by anti-CD162 mAb on cells was quantified. The percentage of neutrophils with adherent platelets decreased from 64 to 3% in the presence of the anti-CD162 mAb, ranging from 1 to 3 particles per FITC-

fluorescent cells [22]. These observations suggest that MIFC can be a useful tool to study in depth the formation of cell aggregates, and their constituents.

The analysis of cell aggregate formation is also relevant in disease settings, such as cell clustering of sickle cells. The sickle cell disease is associated with painful vaso-occlusive crises that occur due to abnormal interactions between endothelial cells, red blood cells and leukocytes. MIFC has been used to study the interaction between red blood cells (RBC) and circulating leukocytes from patients with sickle cell disease or healthy subjects, to evaluate the factors that lead to aggregate formation, which enhance the incidence of vaso-occlusive crises [23]. White blood cells labeled with anti-CD45-FITC and erythrocytes with glycophorin A (GPA)-(PE) conjugated antibodies were mixed and analyzed using MIFC and the IDEAS software. Cell populations were identified by gating on cells expressing surface markers and confirmed by visual inspection of multispectral images. This analysis allowed for the quantitative characterization of single cells or aggregates within a mixed population. In all sickle cell disease patients, a high number of events double positive for both CD45-FITC and GPA-PE was observed, but not in healthy subjects [23]. Cell clusters observed in sickle cell disease patients showed that the double-labeled events corresponded to PBMC aggregates, suggesting that this technology can provide helpful information to analyze the unique constituents of cell aggregates in mixed populations and potentially the disease state of cells like the red blood cells of sickle cell disease [24].

5. Conclusion

The advancement of high-throughput imaging flow cytometry provides a new and powerful tool to the arsenal of technologies available to study cell-cell interaction. Due to the combined capabilities of photometric as well as morphometric analysis of cells on thousands of events, MIFC can be uniquely applied to a number of research and clinical applications. MIFC technology allows researchers the opportunity to combine spatial resolution in multicolor images of cells with the statistical analysis of large number of events through combining the features of fluorescence microscopy and modern flow cytometry in one system. Overall, the applications presented in this chapter are evidence of the broad applications and larger potential of imaging flow cytometry in the field of cell-cell interactions. This technology has also been used successfully in the determination of co-localization of cell surface or nuclear proteins, cell signaling, cell cycle, mitosis analysis, cell death, DNA damage, protein-protein interaction with Forster Resonance Energy Transfer (FRET), intracellular calcium, drug uptake, and pathogen internalization among other uses. It is expected that further advancements of this technology and in the tailoring of fluorophores specifically for these applications will provide deeper insights into this continuously evolving field.

Author details

Cristian Payés and Gustavo Helguera*
School of Pharmacy and Biochemistry, University of Buenos Aires, Argentina

* Corresponding Author

José A. Rodríguez
Molecular Biology Institute, University of California, Los Angeles, CA, USA

Sherree Friend
Amnis – Part of EMD Millipore, Seattle, WA, USA

Acknowledgement

G.H. is supported by the grant PICT-PRH 2008-00315 from Agencia Nacional de Promoción de la Ciencia y Tecnología (ANPCyT) FONARSEC, and by the Grant PIP 114-20110100170 from Consejo Nacional de Investigaciones Científicas y Tecnológicas (CONICET), Argentina. J.A.R. is a Howard Hughes Medical Institute Gilliam fellow and is further funded by the UCLA MBI Whitcome Fellowship. S. F. is employed by Amnis - part of EMD Millipore.

6. References

[1] Okagaki, LH, *et al.*, (2010) Cryptococcal cell morphology affects host cell interactions and pathogenicity. PLoS Pathog. vol. 6, p. e1000953.
[2] Elliott, GS, (2009) Moving pictures: imaging flow cytometry for drug development. Comb Chem High Throughput Screen. vol. 12, pp. 849-59.
[3] Basiji, DA, *et al.*, (2007) Cellular image analysis and imaging by flow cytometry. Clin Lab Med. vol. 27, pp. 653-70, viii.
[4] Basiji, DA, (2007) Multispectral Imaging Flow Cytometry. in 4th IEEE International Symposium on Biomedical Imaging: From Nano to Macro. Arlington, VA. USA.
[5] Kubota, F, *et al.*, (1995) Flow cytometer and imaging device used in combination. Cytometry. vol. 21, pp. 129-32.
[6] Ortyn, WE, *et al.*, (2007) Extended depth of field imaging for high speed cell analysis. Cytometry A. vol. 71, pp. 215-31.
[7] McGrath, KE, *et al.*, (2008) Multispectral imaging of hematopoietic cells: where flow meets morphology. J Immunol Methods. vol. 336, pp. 91-7.
[8] Horner, H, *et al.*, (2007) Intimate cell conjugate formation and exchange of membrane lipids precede apoptosis induction in target cells during antibody-dependent, granulocyte-mediated cytotoxicity. J Immunol. vol. 179, pp. 337-45.
[9] Dall'Ozzo, S, *et al.*, (2004) Rituximab-dependent cytotoxicity by natural killer cells: influence of FCGR3A polymorphism on the concentration-effect relationship. Cancer Res. vol. 64, pp. 4664-9.
[10] Gennari, R, *et al.*, (2004) Pilot study of the mechanism of action of preoperative trastuzumab in patients with primary operable breast tumors overexpressing HER2. Clin Cancer Res. vol. 10, pp. 5650-5.
[11] Helguera, G, *et al.*, (2011) Visualization and quantification of cytotoxicity mediated by antibodies using imaging flow cytometry. J Immunol Methods. vol. 368, pp. 54-63.

[12] Beum, PV, *et al.*, (2008) Binding of rituximab, trastuzumab, cetuximab, or mAb T101 to cancer cells promotes trogocytosis mediated by THP-1 cells and monocytes. J Immunol. vol. 181, pp. 8120-32.
[13] Elishmereni, M, *et al.*, (2011) Physical interactions between mast cells and eosinophils: a novel mechanism enhancing eosinophil survival in vitro. Allergy. vol. 66, pp. 376-85.
[14] Ahmed, F, *et al.*, (2009) Numbers matter: quantitative and dynamic analysis of the formation of an immunological synapse using imaging flow cytometry. J Immunol Methods. vol. 347, pp. 79-86.
[15] Hosseini, BH, *et al.*, (2009) Immune synapse formation determines interaction forces between T cells and antigen-presenting cells measured by atomic force microscopy. Proc Natl Acad Sci U S A. vol. 106, pp. 17852-7.
[16] Hochweller, K, *et al.*, (2010) Dendritic cells control T cell tonic signaling required for responsiveness to foreign antigen. Proc Natl Acad Sci U S A. vol. 107, pp. 5931-6.
[17] Hoffmann, S, *et al.*, (2011) Single cell force spectroscopy of T cells recognizing a myelin-derived peptide on antigen presenting cells. Immunol Lett. vol. 136, pp. 13-20.
[18] Harshyne, LA, *et al.*, (2001) Dendritic cells acquire antigens from live cells for cross-presentation to CTL. J Immunol. vol. 166, pp. 3717-23.
[19] Harshyne, LA, *et al.*, (2003) A role for class A scavenger receptor in dendritic cell nibbling from live cells. J Immunol. vol. 170, pp. 2302-9.
[20] Megjugorac, NJ, *et al.*, (2007) Image-based study of interferongenic interactions between plasmacytoid dendritic cells and HSV-infected monocyte-derived dendritic cells. Immunol Invest. vol. 36, pp. 739-61.
[21] Iype, T, *et al.*, (2010) The protein tyrosine phosphatase SHP-1 modulates the suppressive activity of regulatory T cells. J Immunol. vol. 185, pp. 6115-27.
[22] Ouk, C, *et al.*, (2011) Both CD62 and CD162 antibodies prevent formation of CD36-dependent platelets, rosettes, and artefactual pseudoexpression of platelet markers on white blood cells: a study with ImageStream(R). Cytometry A. vol. 79, pp. 477-84.
[23] Chaar, V, *et al.*, (2010) Aggregation of mononuclear and red blood cells through an {alpha}4{beta}1-Lu/basal cell adhesion molecule interaction in sickle cell disease. Haematologica. vol. 95, pp. 1841-8.
[24] Amer, J and Fibach, E, (2005) Chronic oxidative stress reduces the respiratory burst response of neutrophils from beta-thalassaemia patients. Br J Haematol. vol. 129, pp. 435-41.